Plant Communications
Research article

CellPress
Partner Journal

Synthetic apomixis enables stable transgenerational transmission of heterotic phenotypes in hybrid rice

Chaolei Liu[1,4], Zexue He[2,4], Yan Zhang[1], Fengyue Hu[1], Mengqi Li[2], Qing Liu[1], Yong Huang[1], Jian Wang[1], Wenli Zhang[2,*], Chun Wang[1,*] and Kejian Wang[1,3,*]

[1]State Key Laboratory of Rice Biology, China National Rice Research Institute, Hangzhou 310006, China

[2]State Key Laboratory for Crop Genetics and Germplasm Enhancement, CIC-MCP, Nanjing Agriculture University, Nanjing, Jiangsu 210095, China

[3]Hainan Yazhou Bay Seed Lab, Sanya, Hainan 572025, China

[4]These authors contributed equally to this article.

***Correspondence: Wenli Zhang (wzhang25@njau.edu.cn), Chun Wang (wangchun@caas.cn), Kejian Wang (wangkejian@caas.cn)**

https://doi.org/10.1016/j.xplc.2022.100470

ABSTRACT

In hybrid plants, heterosis often produces large, vigorous plants with high yields; however, hybrid seeds are generated by costly and laborious crosses of inbred parents. Apomixis, in which a plant produces a clone of itself via asexual reproduction through seeds, may produce another revolution in plant biology. Recently, synthetic apomixis enabled clonal reproduction of F_1 hybrids through seeds in rice (*Oryza sativa*), but the inheritance of the synthetic apomixis trait and superior heterotic phenotypes across generations remained unclear. Here, we propagated clonal plants to the T_4 generation and investigated their genetic and molecular stability at each generation. By analyzing agronomic traits, as well as the genome, methylome, transcriptome, and allele-specific transcriptome, we showed that the descendant clonal plants remained stable. Unexpectedly, in addition to normal clonal seeds, the plants also produced a few aneuploids that had eliminated large genomic segments in each generation. Despite the identification of rare aneuploids, the observation that the synthetic apomixis trait is stably transmitted through multiple generations helps confirm the feasibility of using apomixis in the future.

Key words: synthetic apomixis, hybrid rice, transgenerational heredity, stability

Liu C., He Z., Zhang Y., Hu F., Li M., Liu Q., Huang Y., Wang J., Zhang W., Wang C., and Wang K. (2023). Synthetic apomixis enables stable transgenerational transmission of heterotic phenotypes in hybrid rice. Plant Comm. **4**, 100470.

INTRODUCTION

The utilization of heterosis (hybrid vigor) is one of the landmark innovations in modern agriculture. Hybrid varieties of major crops including maize (*Zea mays*), rice (*Oryza sativa*), cotton (*Gossypium hirsutum*), rye (*Secale cereale*), sugar beet (*Beta vulgaris*), and rapeseed (*Brassica napus*) make up a major portion of the global seed market (Hochholdinger and Baldauf, 2018). Farmers prefer to grow hybrids because the first-generation plants exhibit superior performance in traits including yield, quality, adaptability, and biotic and abiotic stress tolerance (Birchler et al., 2010). However, unlike seeds from inbred lines, seeds cannot be harvested from hybrid parents for subsequent generations of production due to variation in their genotypes and phenotypes (Wang, 2020). Therefore, hybrid seeds must be produced annually, which is a laborious, costly, and environmentally sensitive task, making hybrid seeds more expensive than inbred seeds (Underwood and Mercier, 2022). Therefore, breeders and geneticists are eager to explore approaches to fixing heterosis in hybrid lines for several generations.

Apomixis is a form of reproduction that produces seeds containing a set of genes identical to that of the maternal parent. However, major crop species lack this valuable agricultural trait (Calzada et al., 1996). In more than 400 natural apomictic species, apomictic seed development consists of three distinct steps: the formation of unreduced female gametophytes, parthenogenesis, and functional endosperm development (Kaushal et al., 2019). Notably, due to the suppressed recombination and polyploidy of apomictic species, the genetic

Published by the Plant Communications Shanghai Editorial Office in association with Cell Press, an imprint of Elsevier Inc., on behalf of CSPB and CEMPS, CAS.

control of natural apomixis is difficult to study and has remained obscure (Ozias-Akins and van Dijk, 2007; Ozias-Akins and Conner, 2020). The *PsASGR-BABY BOOM-like* gene is the first parthenogenesis gene cloned from *Pennisetum squamulatum* (Conner et al., 2015), and introduction of the *PsASGR-BABY BOOM-like* gene into rice and maize conferred the ability to induce haploid embryos (Conner et al., 2017). The apomictic *PARTHENOGENESIS* allele was recently identified in dandelion (*Taraxacum officinale*) and was shown to initiate parthenogenesis in lettuce (*Lactuca sativa*) (Underwood et al., 2022). The identification of these two apomictic genes offers great promise for use in major crops. Although extensive efforts have been made in the field in recent decades, attempts to introduce natural apomixis traits into major crops have thus far been unsuccessful (Wang, 2020).

Synthetic apomixis produced by molecular engineering offers tremendous potential to fix hybrid vigor in crops. The *mitosis instead of meiosis (MiMe*) strategy, which converts meiosis into mitosis and generates clonal gametes, was successfully employed in flowering plants, representing the first step in establishing synthetic apomixis in crop species (d'Erfurth et al., 2009; Mieulet et al., 2016). Subsequently, the sperm-specific phospholipase MATRILINEAL (MTL) was shown to trigger haploid seed production in cereals (Kelliher et al., 2017; Yao et al., 2018; Liu et al., 2020). In addition, ectopic expression of the male-expressed gene *BABY BOOM1* in egg cells was demonstrated to be sufficient for parthenogenesis (Khanday et al., 2019). By crossing *MiMe* plants with the *CENH3*-mediated genome-elimination lines, clonal seeds were successfully obtained in *Arabidopsis* (Marimuthu et al., 2011). Recently, a synthetic apomixis system was developed in rice by combining *MiMe* with *BABY BOOM1* or *MTL* (Khanday et al., 2019; Wang et al., 2019; Xie et al., 2019). Although synthetic apomixis was successfully performed in rice, some important issues remain to be addressed before apomixis can be used in the field (Underwood and Mercier, 2022).

The stable transmission of synthetic apomixis is essential for its application in agriculture (Sailer et al., 2016). However, whether the synthetic apomixis trait can be transferred stably between different generations in hybrid plants remains unknown. In the current study, we assessed the heritability of this trait by examining clonal *fixation of hybrids (Fix*) plants that we advanced from the T_0 to the T_4 generation.

RESULTS AND DISCUSSION

Fix progenies have no obvious phenotypic changes

We previously fixed the heterozygosity of F_1 hybrid rice by mutating the three *MiMe* genes and the *MTL* gene in the elite inter-subspecific hybrid rice variety Chunyou 84 (CY84) (Wang et al., 2019). The *osd1 pair1 rec8 mtl* quadruple mutant (named *Fix*) displayed a phenotype similar to that of CY84, except for a low seed-setting rate, and generated 6.2% clonal *Fix* and 93.8% tetraploid seeds (number of clonal seeds/number of progeny tested) (Wang et al., 2019). In the current study, to examine whether inheritance of the synthetic apomixis trait was stable, we accelerated the generation of *Fix* plants and advanced the population from the T_0 to the T_3 generation in four continuous seasons (Figure 1A). We determined the ploidy level of the progeny seedlings from *Fix* plants of different generations (T_0, T_1, T_2, and T_3) using flow cytometry and identified individuals with three types of ploidy: diploids (2n = 2x), tetraploids (2n = 4x), and aneuploids (2x < 2n < 4x) (Figure 1B). The representative results of diploids and tetraploids are shown in Supplemental Figure 1. We initially focused on diploid *Fix* plants. In total, we identified 17, 20, 14, and 11 diploids out of 885, 664, 518, and 345 progeny individuals from *Fix* plants of the T_0, T_1, T_2, and T_3 generations, with 1.9%, 3%, 2.7%, and 3.2% clonal seed rates, respectively (Figure 1B). The average clonal seed rate of the *Fix* clonal plants was 2.6%, which was lower than the previously reported value of 6.2% (Wang et al., 2019), suggesting that the trait might be susceptible to the external environment. The descendant diploids of different generations (labeled *Fix*–T_1, –T_2, –T_3, and –T_4 hereafter), as well as *Fix*–T_0 and CY84, were planted in the field to evaluate the stability of synthetic apomixis (Figure 1).

To investigate whether any changes occurred in the progeny plants, we compared the agronomic traits of CY84, *Fix*–T_0, *Fix*–T_1, *Fix*–T_2, *Fix*–T_3, and *Fix*–T_4 diploid plants along with their corresponding tetraploid lines. The diploid plants displayed similar agronomic traits, based on heading date, tiller number, plant height, panicle length, grain number per panicle, and 1000-grain weight (Figure 2A–2F). Although the seed-setting rate of the *Fix* clonal plants was drastically reduced (5.7%–7%) compared with that of the hybrid rice line CY84 (75.9%), this value was nearly identical among *Fix* plants from all generations (Figure 2G). The clonal seed rates were 3.7% (*Fix*–T_0), 4% (*Fix*–T_1), 3.3% (*Fix*–T_2), 3% (*Fix*–T_3), and 4.3% (*Fix*–T_4) (Figure 2H; Supplemental Table 1), indicating that the synthetic apomixis trait is transmitted to subsequent generations and remains stable over multiple generations. In addition, there were no significant differences in plant or panicle morphology among the tetraploid plants from the T_1, T_2, T_3, and T_4 generations (Supplemental Figures 1–3). Therefore, the *Fix* offspring, including both diploids and tetraploids, exhibited no obvious changes over multiple generations, and the clonal progeny plants maintained hybrid vigor based on their phenotypes.

Whole-genome, methylome, and transcriptome analyses reveal the high stability of the synthetic apomixis system over multiple generations

We asked whether heterozygosity remained fixed in the advanced generations of apomictic plants by performing whole-genome sequencing of CY84, *Fix*–T_0, *Fix*–T_1, *Fix*–T_2, *Fix*–T_3, and *Fix*–T_4 plants. A total of 43 720 008–55 159 928 reads were captured, >95% of which were mapped to the reference genome (Supplemental Table 2). We performed correlation analyses of the whole-genome sequencing data and found high uniformity among these data sets (0.94–0.99) (Supplemental Figure 4). Bioinformatic analysis using 78 909 previously reported single-nucleotide polymorphisms (SNPs) between 16A and C84 (Wang et al., 2019) showed that each genome had a high density and good distribution of SNPs on the 12 chromosomes and exhibited heterozygosity on every chromosome (Figure 3A). Therefore, the whole genomes of CY84, *Fix*–T_0, *Fix*–T_1, *Fix*–T_2, *Fix*–T_3, and *Fix*–T_4 are all genetically identical (Figure 3B), suggesting that the synthetic

A

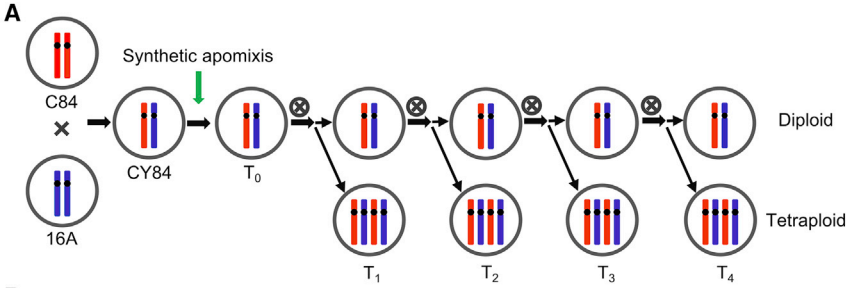

B

Generation	Progeny tested	Diploid	Tetraploid	Aneuploid	Clonal seed rate
T_0	885	17	866	2	1.9 %
T_1	664	20	641	3	3.0 %
T_2	518	14	502	2	2.7 %
T_3	345	11	331	3	3.2 %

Figure 1. Generation of multiple generations of *Fix* clonal plants.

(A) Schematic diagram of the method used to create multiple generations of *Fix* clonal materials. *Fix* was accelerated from the T_0 to the T_3 generation in four continuous seasons, and the multiple generations of *Fix* plants (T_0 to T_4), as well as CY84, were then evaluated in the same season.

(B) Ploidy analysis of the progeny of *Fix* plants from four generations. The identified diploid, tetraploid, and aneuploid plants were grown in the field for evaluation in the same season.

apomixis trait is transferred over multiple generations and is stable at the whole-genome level.

To determine whether any epigenetic changes occurred among different generations of apomictic plants, we performed whole-genome bisulfite sequencing (BS-seq) of *Fix* plants from different generations and CY84. We generated 35.7–51.6 million paired-end BS-seq reads, ~67% of which were uniquely mapped to the reference genome (Supplemental Table 3). Correlation and clustering analysis of the BS-seq data revealed high Pearson's correlation coefficients (0.96–0.99) between *Fix* clonal progeny (*Fix*–T_1 to *Fix*–T_4), *Fix*–T_0, and CY84 (Supplemental Figure 5). We further defined differentially methylated regions in CG, CHG, and CHH contexts by comparing genome-wide methylation statuses from different libraries. In brief, a relatively low number of CG, CHG, and CHH hypermethylation/hypomethylation differentially methylated regions were identified among the *Fix* and CY84 plants (Supplemental Table 4). These results indicate that the methylation landscape likely remains stable over the course of transfer of the synthetic apomixis trait.

We also explored the CG, CHG, and CHH status at both genes and transposable elements (TEs). Consistent with a previous report (Feng et al., 2010), we detected one peak in CG methylation levels within gene body regions, flanked by two valleys around the transcriptional start and termination sites (Figure 3C). By contrast, the gene body regions showed reduced CHG and CHH methylation levels compared with the upstream and downstream regions (Figure 3C). The CG and CHG methylation levels of TEs were much higher than those of genes, but CHH methylation levels in TEs and genes were similar (Figure 3C). Importantly, although the CG, CHG, and CHH methylation levels of CY84 were slightly higher than those of *Fix*-T_0 plants, we observed no significant differences (Wilcoxon test) in methylation levels between *Fix*–T_0 and all *Fix* clonal progeny plants (Figure 3C; Supplemental Figures 6 and 7). These results suggest that the transfer of the synthetic apomixis trait has no obvious effect on the methylome.

We then examined the effects of transfer of the synthetic apomixis trait on gene expression patterns from flag leaves. To facilitate the exploration of transcriptome changes, we introduced four generations of the Nipponbare variety (abbreviated NIP1st, -2nd, -3rd, and -4th) as a control. Total RNA was isolated from flag leaves and used to generate RNA sequencing (RNA-seq) data. We obtained an average of 17.5 million RNA-seq reads, ~97% of which mapped to the reference genome (Supplemental Table 5). Correlation and clustering analysis underscored the high uniformity of the expression profiles obtained for the synthetic apomixis group (0.93–1.00) (Supplemental Figure 8) and the Nipponbare control group (0.90–0.99) (Supplemental Figure 9A). Transcriptome analysis resulted in >23 600 genes for each comparison in the synthetic apomixis group (Supplemental Figure 10) and >22 500 genes for the Nipponbare control group (Supplemental Figure 9B), which formed the dataset for subsequent analyses. Comparisons of gene expression levels showed that no more than 0.5% of genes were differentially expressed in each comparison in the synthetic apomixis group, and no more than 1% of genes were differentially expressed in each comparison over the four generations of Nipponbare (adjusted $p < 0.05$ and $|\text{Log}_2[\text{fold change}]| > 1$) (Figure 3D). Collectively, these results indicate that gene-expression patterns are not significantly altered across different generations of *Fix* plants.

Fix offspring plants exhibit highly stable allele-specific transcriptomes

Hybridization can initiate transcriptomic shock, a phenomenon whereby hybrids exhibit radically altered gene-expression patterns relative to their parents (Hegarty et al., 2006). CY84 is an elite inter-subspecific hybrid rice from a cross between 16A (a *japonica* male-sterile line) and C84 (an *indica–japonica* intermediate-type line), which has likely undergone transcriptomic shock. To explore the effects of the transfer of synthetic apomixis on allele-specific gene expression, we extracted the expression levels of each parental allele via RNA-seq analysis of CY84, *Fix*–T_0, *Fix*–T_1, *Fix*–T_2, *Fix*–T_3, and *Fix*–T_4 plants using the different SNPs between the 16A and C84 genomes (Wang et al., 2019). Using a previously reported method (Xu et al., 2014), we identified 10 211–10 419 genes harboring diagnostic SNPs between 16A and C84 for analysis (Supplemental Figure 11). Plotting the $\log_2$(FPKM + 1) (where FPKM is fragments per kilobase of transcript per million mapped reads) values derived from each allele across all plants revealed a significant difference (Wilcoxon test) in parental expression

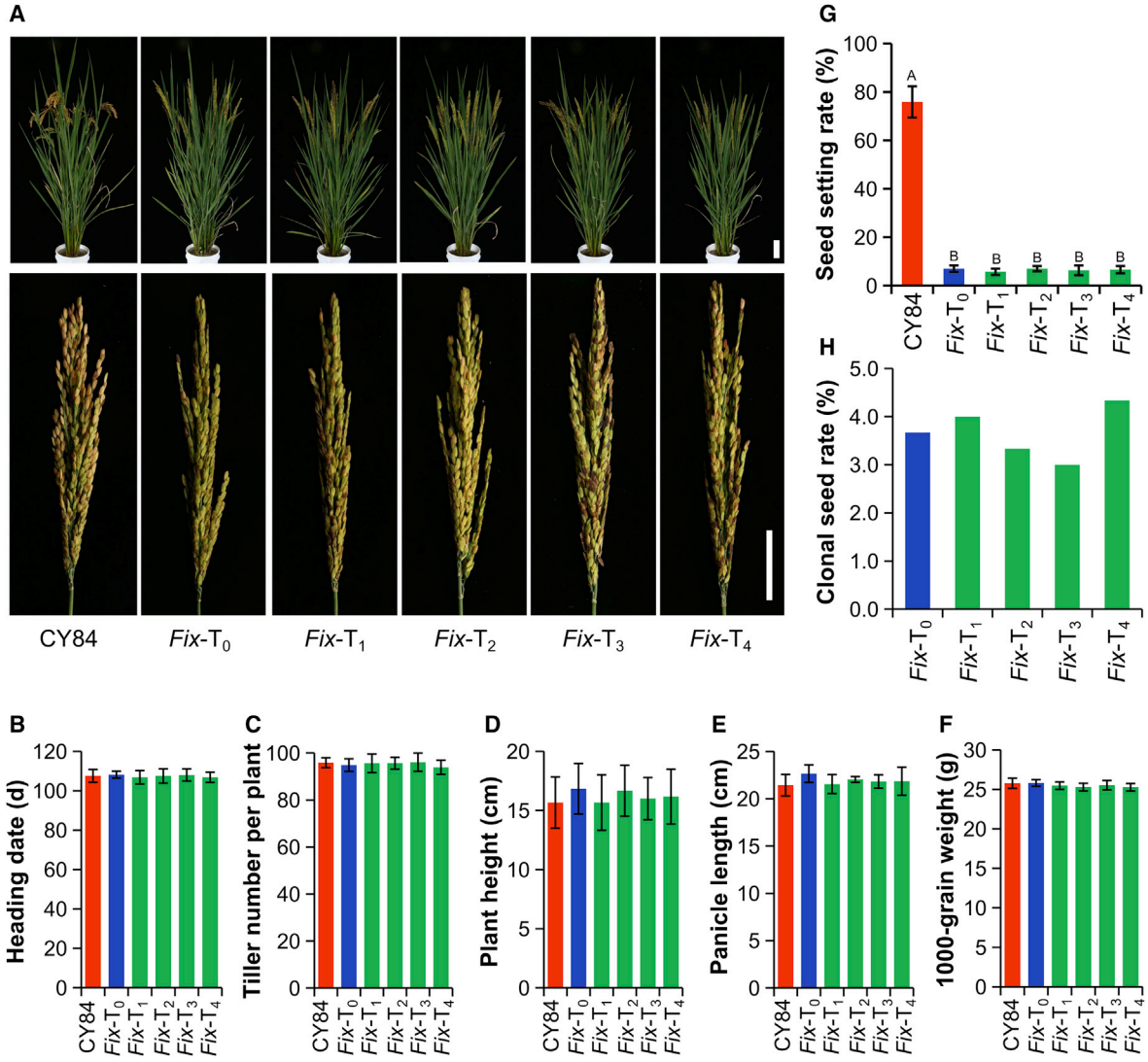

Figure 2. Phenotypic comparison of multiple generations of *Fix* clonal plants.

(A) Plant morphology (top panel) and panicles (bottom panel) of CY84, *Fix*–T_0, *Fix*–T_1, *Fix*–T_2, *Fix*–T_3, and *Fix*–T_4. The plants were grown in paddy fields in Hangzhou. Scale bars, 20 cm (top panel) or 5 cm (bottom panel).

(B–H) Heading date **(B)**, tiller number per plant **(C)**, plant height **(D)**, panicle length **(E)**, 1000-grain weight **(F)**, seed setting rate **(G)**, and clonal seed rate **(H)** of CY84, *Fix*–T_0, *Fix*–T_1, *Fix*–T_2, *Fix*–T_3, and *Fix*–T_4 plants. Data are means ± SD ($n \geq 6$); different letters indicate a significant difference at the 1% level according to Tukey's test.

levels in CY84, *Fix*–T_0, *Fix*–T_1, *Fix*–T_2, *Fix*–T_3, and *Fix*–T_4 (Figure 4A), suggesting that transcriptomic shock indeed occurred in CY84 and was maintained and fixed in the progeny plants.

In addition, more than 60% of genes were differentially expressed between the two parental alleles in each sample (ratio of 16A and C84 allele expression ≠ 1:1, Wilcoxon test), with 6421–6483 upregulated genes and 6715–6884 downregulated genes (Figure 4B). A comparison of 16A and C84 allele-specific gene expression levels in CY84, *Fix*–T_0, *Fix*–T_1, *Fix*–T_2, *Fix*–T_3, and *Fix*–T_4 showed that, at most, nine genes were differentially expressed in each comparison (Figure 4C). When we plotted the $\log_2$(FPKM[16A]/FPKM[C84]+1) expression ratios of the 10 211–10 419 genes in each plant sample as a boxplot, we detected no significant differences (Wilcoxon test) among CY84, *Fix*–T_0, *Fix*–T_1, *Fix*–T_2, *Fix*–T_3, or *Fix*–T_4 (Figure 4D). These results suggest that the transmission of the synthetic apomixis trait has no distinct influence on the allele-specific transcriptome.

Identification of aneuploid plants in the *Fix* offspring

Unexpectedly, besides diploids and tetraploids, we also identified 2, 3, 2, and 3 aneuploid plants ($2x < n < 4x$) in the progeny individuals of *Fix* plants from the T_0, T_1, T_2, and T_3 generations, corresponding to rates of 0.22%, 0.45%, 0.38%, and 0.86%, respectively (Figures 1B and 5A). Only four aneuploid plants survived when grown in the paddy field. We sequenced the genomes of these four remaining aneuploids and determined that three types of large genomic deletions had occurred (Figure 5B): type I, aneuploid plants $^{\#}2$ and $^{\#}4$ lost one copy of seven and three chromosomes, respectively; type

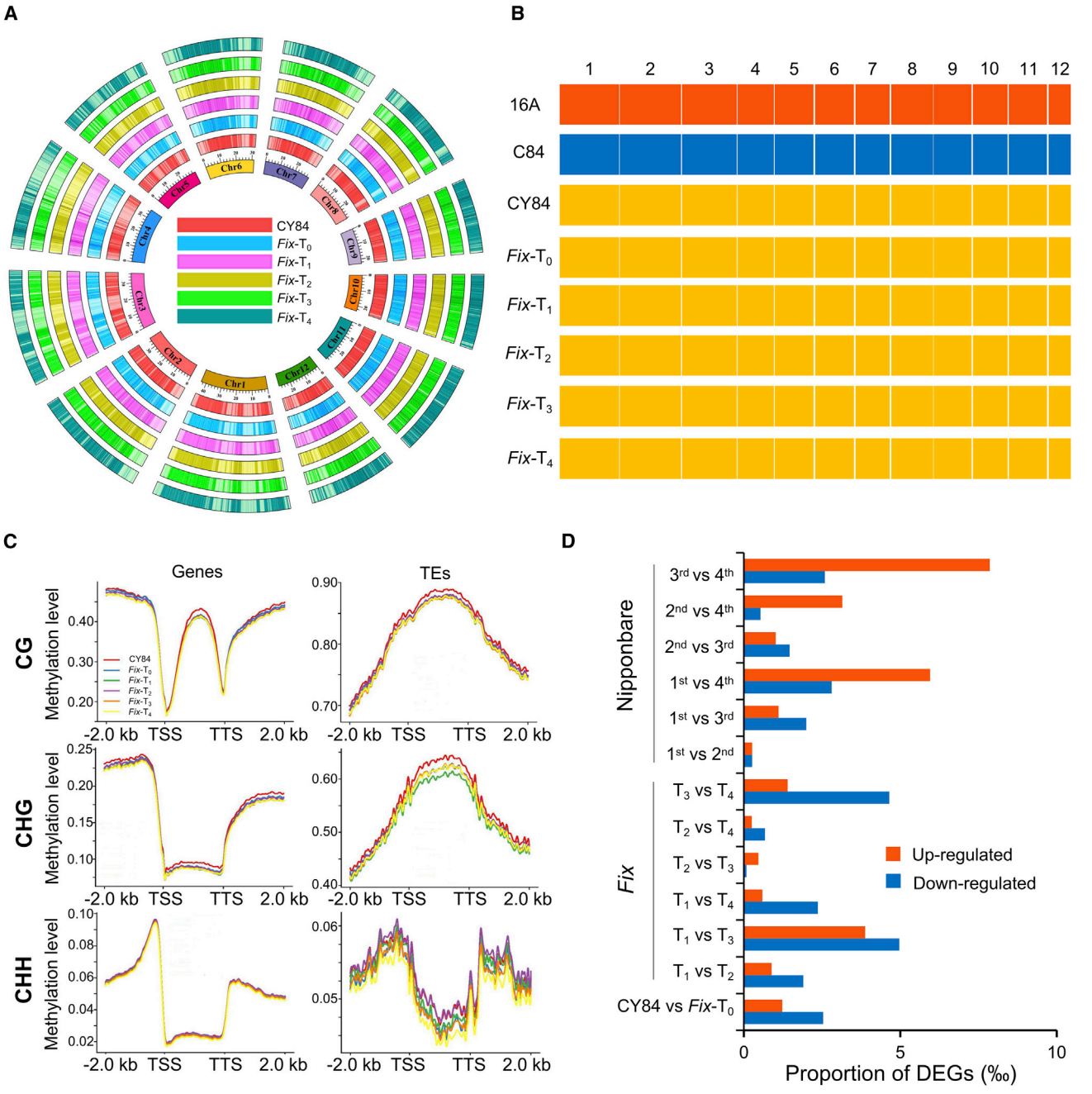

Figure 3. Genome, methylome, and transcriptome analysis of multiple generations of *Fix* clonal plants.

(A) Whole-genome sequencing of CY84, *Fix*–T_0, *Fix*–T_1, *Fix*–T_2, *Fix*–T_3, and *Fix*–T_4. The distribution of SNPs on 12 chromosomes is shown in a circos plot.

(B) *Fix*–T_0, *Fix*–T_1, *Fix*–T_2, *Fix*–T_3, and *Fix*–T_4 are heterozygous and identical to CY84. Red, C84 SNP allele; blue, 16A SNP allele; yellow, both alleles are present. The 12 blocks represent the 12 rice chromosomes.

(C) Distribution of the average methylation level over gene or transposable element bodies and the 2 kb of flanking sequence on each side. TSS and TTS indicate the transcription start site and transcription termination site.

(D) Percentage of differentially expressed genes in each comparison between the synthetic apomixis group and the Nipponbare control group. The proportion of differentially expressed genes equals the number of differentially expressed genes/total number of mapped genes.

II, aneuploid #3 harbored deletions of segments from chromosomes 1, 2, and 5; and type III, aneuploid #1 exhibited both loss of entire chromosome copies and deletions of chromosomal segments (Figure 5B and 5C). The random elimination of chromosomes or chromosomal segments had disastrous effects on plant growth and development. All four aneuploid plants displayed decreased plant height, short panicles, and absolute sterility compared with *Fix* diploid and tetraploid plants when planted in paddy fields (Figure 5D and 5E). In addition, the seeds from aneuploid plants #2 and #3 had long awns (Figure 5E), perhaps due to the extra genome copies compared with the diploids.

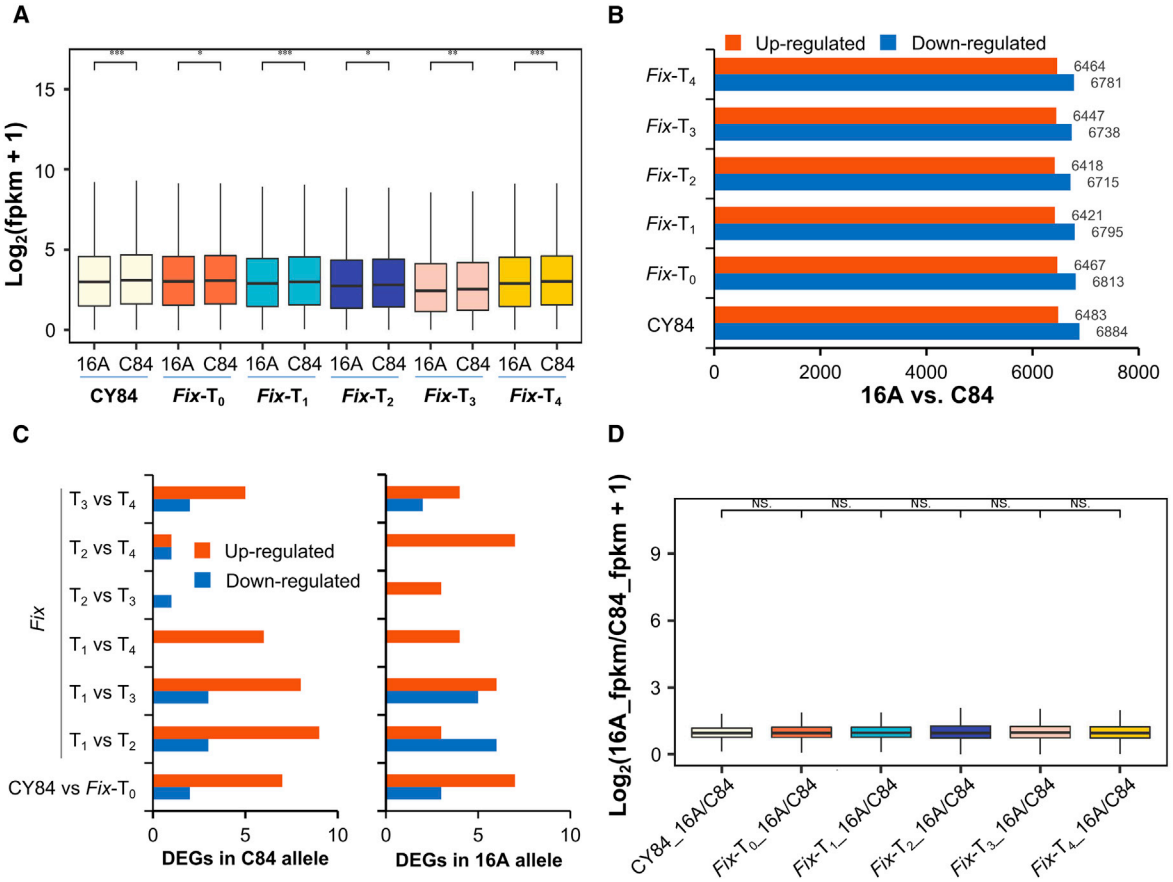

Figure 4. Allele-specific transcriptome analysis over multiple generations of *Fix* clonal plants.

(A) RNA–seq-based global expression spectra of C84 and 16A allelic expression divergence in CY84, *Fix*–T_0, *Fix*–T_1, *Fix*–T_2, *Fix*–T_3, and *Fix*–T_4. *$p < 0.05$; **$p < 0.01$; ***$p < 0.001$ (Wilcoxon test).

(B) Number of genes showing differential expression between the 16A and C84 alleles in CY84, *Fix*–T_0, *Fix*–T_1, *Fix*–T_2, *Fix*–T_3, and *Fix*–T_4.

(C) The number of differentially expressed genes in each pairwise comparison in the C84 and 16A allele, respectively.

(D) Specific values of 16A/C84 allele-level RNA-seq data among CY84, *Fix*–T_0, *Fix*–T_1, *Fix*–T_2, *Fix*–T_3, and *Fix*–T_4. NS, no significant difference (Wilcoxon test).

Previous studies in *Arabidopsis* revealed that aneuploids can be induced by *MiMe-2* (*spo11-1 rec8 tam*) (d'Erfurth et al., 2010). Similarly, aneuploids were also observed when crossing wild-type *Arabidopsis* plants with *CENH3*-mediated genome-elimination lines (Tan et al., 2015). The *Fix* strategy in this study was artificially implemented by combining *MiMe* with *MTL* (Wang et al., 2019). To explore whether the aneuploids of *Fix* were caused by *MiMe* or *MTL*, we analyzed the ploidy levels of the progenies of *MiMe* (*pair1 rec8 osd1*) and *mtl* plants. A total of 276 progenies of *MiMe* were analyzed, and all plants were found to be tetraploids, which was consistent with previous studies (Mieulet et al., 2016; Wang et al., 2019). Of 305 progenies of *mtl* plants, 19 haploids and 286 diploids were found. The absence of aneuploid offspring from *mtl* plants is consistent with previous observations in maize, rice, and wheat (Gilles et al., 2017; Kelliher et al., 2017; Liu et al., 2017, 2020; Yao et al., 2018; Jiang et al., 2022). However, although no aneuploid offspring were identified, investigations in maize revealed that continuous large-scale chromosome fragmentation occurred in the *mtl* gametophyte (Li et al., 2017). Considering the nearly normal seed set of *MiMe* plants but significantly reduced seed production of *mtl* and *Fix*, we favor the idea that the aneuploid offspring of *Fix* might be caused by incomplete genome elimination by the *MTL* mutation. In addition, tetraploid plants might be more tolerant of genome incompleteness than normal diploid rice. Therefore, some aneuploid plants survived in the offspring of *Fix* but not the offspring of *mtl* (Supplemental Figure 12). Of course, we cannot exclude the possibility that aneuploid offspring of *Fix* might be caused by incomplete penetrance of *MiMe* gametes (d'Erfurth et al., 2010) or by few haploid female gametes of *Ososd1* (Mieulet et al., 2016). In the future, further studies will be required to clarify the underlying mechanisms of aneuploid formation.

In this study, we investigated the stability of inheritance of synthetic apomixis across multiple clonal generations, an important issue in the apomixis field. Our studies of several generations of *Fix* clonal progeny revealed the stability of the synthetic apomixis trait in terms of plant morphology as well as the genome, methylome, transcriptome, and allele-specific transcriptome. Although a low frequency of aneuploid plants was observed, the genetic and molecular stability of the *Fix* plants demonstrates the feasibility of using synthetic apomixis in the future.

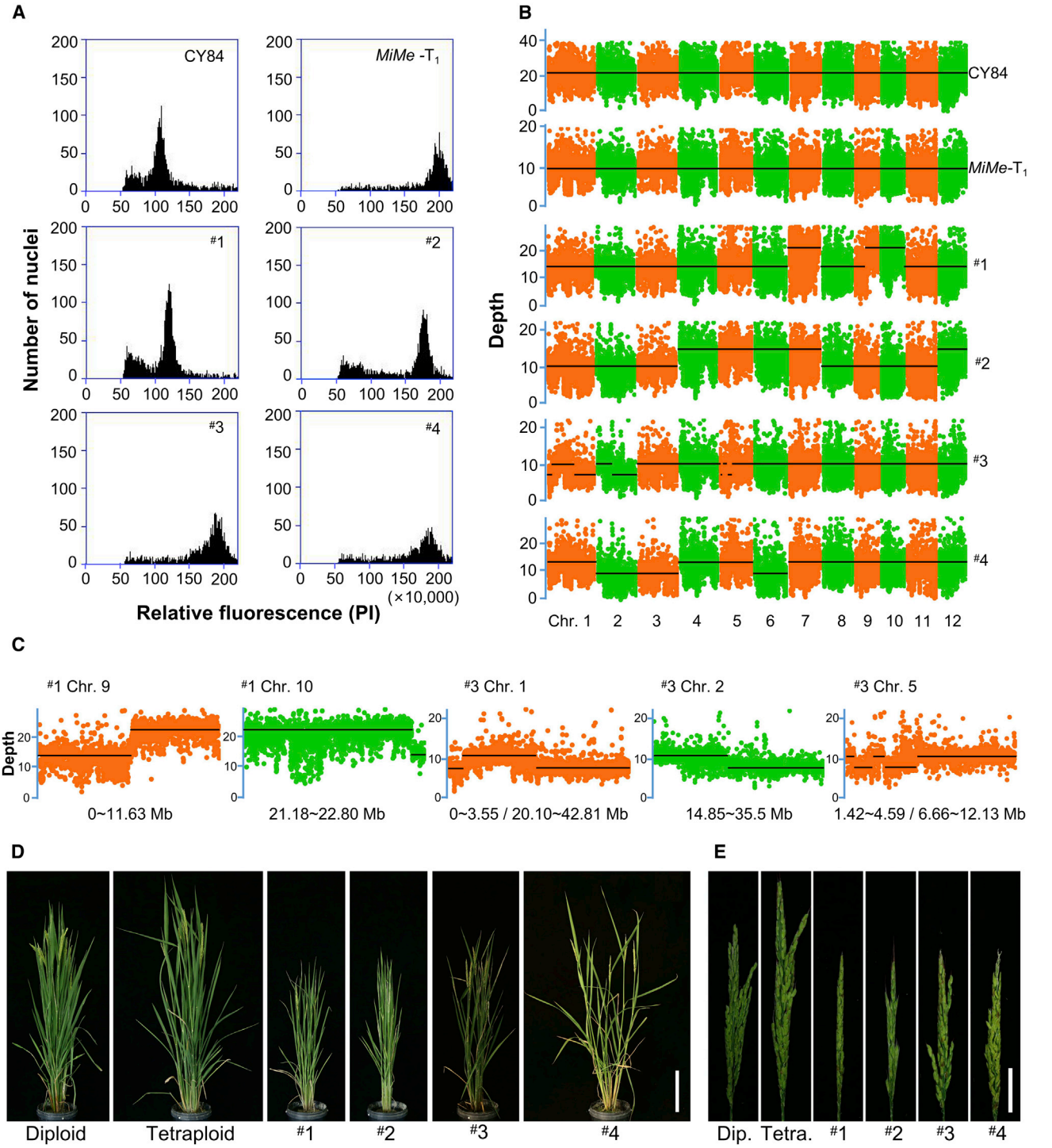

Figure 5. Characterization of aneuploid plants induced by the synthetic apomixis system.

(A) Ploidy levels of aneuploid plants, as determined by flow cytometry. PI, propidium iodide.

(B) Whole-genome sequencing of CY84 (control 1), *MiMe*–T_1 (control 2), and aneuploid plants $^{\#}1$, $^{\#}2$, $^{\#}3$, and $^{\#}4$.

(C) Aneuploid plants $^{\#}1$ and $^{\#}3$ have abnormal chromosomes. Some fragments on chromosomes 9 and 10 (aneuploid $^{\#}1$) and on chromosomes 1, 2, and 5 (aneuploid $^{\#}3$) were deleted.

(D) Plant morphology of diploid (control 1), tetraploid (control 2), and aneuploid plants $^{\#}1$, $^{\#}2$, $^{\#}3$, and $^{\#}4$. Scale bars, 20 cm.

(E) Panicles of diploid (control 1), tetraploid (control 2), and aneuploid plants $^{\#}1$, $^{\#}2$, $^{\#}3$, and $^{\#}4$. The plants were grown in paddy fields in Hangzhou. Scale bars, 4 cm.

METHODS

Plant materials and growth conditions

The *Fix* (T_0 generation) plants were previously generated in the hybrid rice CY84 genetic background, an elite inter-subspecific hybrid rice derived from a cross between the maternal line Chunjiang 16A (16A), a *japonica* male-sterile line, and the paternal line C84, an *indica–japonica* intermediate-type line (Wang et al., 2019). The *Fix* plants were self-pollinated from the T_0 to the T_3 generation, and diploids were screened at each generation. The *Fix* (T_0 generation) and CY84 (corresponding control for the T_0 generation *Fix*) plants were preserved to the next generation via ratoon. Seeds from the *Fix* plants (*Fix* from T_0, T_1, T_2, and T_3 generation; *Fix*–T_0, –T_1, –T_2, –T_3, and –T_4), *MiMe*–T_0, and the Nipponbare cultivar (continuously self-pollinated for four generations, designated Nip1st, -2nd, -3rd, and -4th) were soaked in deionized water at 37°C in the dark for 2 days, transferred to a net floating on deionized water, and incubated for 5 days. The seedlings were cultured in half-strength Kimura B nutrient solution (pH 5.4) for 21 days. The ploidy levels of *Fix* progeny seedlings were identified by flow cytometry as described below. All confirmed seedlings were transferred to a paddy field in Hangzhou, China. Plant growth in the field was managed according to local cultivation practices.

Characterization of agronomic traits

To compare the agronomic traits of *Fix*–T_0, CY84, and *Fix* progeny (*Fix*–T_1, *Fix*–T_2, *Fix*–T_3, and *Fix*–T_4), the plants were grown to maturity in the paddy field. The dates of sowing and heading were used to calculate the heading date (in days). Measurements of tiller number and plant height were performed directly in the field at 25 days after heading. Then, the main panicles were harvested to measure panicle length in the laboratory.

Flow cytometry to determine plant ploidy

The ploidy level of each line was determined by estimating nuclear DNA contents using flow cytometry. Approximately 2-cm^2 samples of leaf tissue were chopped in 1 mL LB01 buffer (15 mM Tris, 2 mM disodium EDTA, 0.5 mM spermine tetrahydrochloride, 80 mM KCl, 20 mM NaCl, 0.1% (v/v) Triton X-100, 15 mM β-mercaptoethanol [pH 7.5], filtered through a 0.22-μm filter) on ice using a new razor blade. The homogenate was filtered through a 40-μm nylon mesh, and the nuclei were collected by centrifugation at 4°C (135 × *g*, 5 min). The supernatant was discarded, and the pellet was resuspended in 450 μL fresh LB01 buffer. To stain the DNA, 25 μL 1 mg/mL propidium iodide and 25 μL 1 mg/mL DNase-free RNase A were added to each sample. The samples were incubated on ice in the dark for 10 min and analyzed using a BD Accuri C6 flow cytometer with laser illumination at 552 nm and a 610/20 nm filter (Wang et al., 2019).

BS-seq and analysis of methylation data

The same exact plants of synthetic apomixis materials were used for DNA sequencing, BS-seq, and RNA-seq. Flag leaves were obtained from the clonal *Fix* progeny (*Fix*–T_1, *Fix*–T_2, *Fix*–T_3, and *Fix*–T_4), *Fix*–T_0, and CY84 at heading and ground to a fine powder in liquid nitrogen using a mortar and pestle. Genomic DNA was isolated from the samples using a Plant Genomic DNA Purification Kit (Tiangen, Beijing, China) and sent to GENEWIZ (Suzhou, China) for bisulfite treatment, library preparation, and next-generation sequencing on the Illumina HiSeq 2000 platform (Illumina, San Diego, CA, USA).

The fastp tool (v.0.21.0) was used to estimate the raw reads and assess their quality. Low-quality reads and adapters were removed from the raw data using fastp, and the clean data were mapped to the rice reference genome (MSU7.0) using Bismark (v.0.23.0). Uniquely mappable reads were used to calculate the methylated cytosines using the Bismark methylation extractor program. The DNA methylation level at each cytosine was estimated only when the total number of all C + T bases counted for that position was at least 5. The methylation ratio for each single cytosine nucleotide was calculated as the number of unconverted cytosines divided by the total number of uniquely mappable reads at each targeted locus. To calculate DNA methylation levels in different regions, we split each region into small windows (20 bp each), and the DNA methylation levels were calculated by averaging the DNA methylation ratios of all cytosine sites within each window.

RNA-seq and data analysis

Flag leaves were obtained at heading from the clonal *Fix* progeny (*Fix*–T_1, *Fix*–T_2, *Fix*–T_3, and *Fix*–T_4), *Fix*–T_0, CY84, and four generations of Nipponbare (Nip1st, -2nd, -3rd, and -4th) and ground to a fine powder in liquid nitrogen using a mortar and pestle. Total RNA was isolated from the samples using TRIzol reagent (15596026; Invitrogen, Waltham, MA, USA) and sent to GENEWIZ for RNA-seq library construction and sequencing on the Illumina HiSeq 2000 platform.

For RNA-seq data analysis, raw reads in fastq format were processed. FastQC was used to estimate the raw reads and assess their quality. Trimming of reads was performed in Trimmomatic (v.0.39), and reads containing contaminating primers/adapters and long stretches of poor-quality bases were removed. An index of the reference genome was built using HISAT2 (v.2.1.0) (Kim et al., 2015), and paired-end clean reads were aligned to the reference genome using HISAT2. The mapped reads from each sample were assembled by StringTie (v.1.3.4d) using a reference-based approach (Pertea et al., 2015). FeatureCounts (v.1.6.4) was used to count the number of reads mapping to each gene. The FPKM value of each gene was calculated based on the length of the gene and read counts mapped to the gene. Differential expression analysis of two conditions/groups (two biological replicates per condition) was performed using the DESeq2 R package (1.30.1). Genes with an adjusted $p < 0.01$ and $|\text{Log}_2(\text{fold change})| > 1$, as determined by DESeq2, were considered differentially expressed genes.

The separation and comparison of allele-level RNA-seq reads were performed as previously described (Xu et al., 2014). A list of SNPs between 16A and C84 from our previous study (Wang et al., 2019) was used for separation of allele-level RNA-seq reads. An "N-masked" genome was then constructed by replacing these SNPs with "N" to reduce mapping bias, and all clean RNA-seq reads were mapped to the masked pseudogenome. The BAM files were submitted to SNPsplit software to separate 16A-specific and C84-specific reads based on the base information at SNP sites. Allele-specific RNA-seq data analysis was performed as described above.

Whole-genome resequencing

Flag leaves from CY84, *Fix*–T_0, *Fix*–T_1, *Fix*–T_2, *Fix*–T_3, *Fix*–T_4, *MiMe*–T_1, and aneuploid plants #1, #2, #3, and #4 were obtained at heading and ground to a fine powder in liquid nitrogen using a mortar and pestle. Genomic DNA was isolated from the samples using a Plant Genomic DNA Purification Kit (Tiangen) and sent to GENEWIZ for library preparation and next-generation sequencing on the Illumina HiSeq 2000 platform (Illumina) to an average depth of approximately 10- to 30-fold coverage for each sample.

FUNDING

This work was supported by the National Natural Science Foundation of China (U20A2030, 32025028, and 32188102); the Central Public-interest Scientific Institution Basal Research Fund (Y2022QC20); the Hainan Yazhou Bay Seed Laboratory (#B21HJ0215); and the Agricultural Science and Technology Innovation Program of the Chinese Academy of Agricultural Sciences (CAAS-ZDRW202001).

DATA AVAILABILITY

All omics data generated in this study have been deposited in the NCBI SRA database. The accession number is NCBI: PRJNA883764 (https://www.ncbi.nlm.nih.gov/bioproject/PRJNA883764/).

SUPPLEMENTAL INFORMATION

Supplemental information is available at *Plant Communications Online*.

ACKNOWLEDGMENTS

No conflict of interest is declared.

AUTHOR CONTRIBUTIONS

K.W., C.W., W.Z., and C.L. managed the project. C.L., Z.H., Y.Z., F.H., M.L., Y.H., and J.W. performed the experiments. C.L., Z.H., and Q.L. analyzed the data. C.L. wrote the manuscript. K.W. revised the manuscript.

Received: July 14, 2022
Revised: September 28, 2022
Accepted: October 29, 2022
Published: November 2, 2022

REFERENCES

Birchler, J.A., Yao, H., Chudalayandi, S., Vaiman, D., and Veitia, R.A. (2010). Heterosis. Plant Cell. **22**:2105–2112.

Calzada, J.P.V., Crane, C.F., and Stelly, D.M. (1996). Apomixis–the asexual revolution. Science **274**:1322–1323.

Conner, J.A., Mookkan, M., Huo, H., Chae, K., and Ozias-Akins, P. (2015). A parthenogenesis gene of apomict origin elicits embryo formation from unfertilized eggs in a sexual plant. Proc. Natl. Acad. Sci. USA **112**:11205–11210.

Conner, J.A., Podio, M., and Ozias-Akins, P. (2017). Haploid embryo production in rice and maize induced by *PsASGR-BBML* transgenes. Plant Reprod. **30**:41–52.

d'Erfurth, I., Cromer, L., Jolivet, S., Girard, C., Horlow, C., Sun, Y., To, J.P.C., Berchowitz, L.E., Copenhaver, G.P., and Mercier, R. (2010). The cyclin-A CYCA1;2/TAM is required for the meiosis I to meiosis II transition and cooperates with OSD1 for the prophase to first meiotic division transition. PLoS Genet. **6**, e1000989.

d'Erfurth, I., Jolivet, S., Froger, N., Catrice, O., Novatchkova, M., and Mercier, R. (2009). Turning meiosis into mitosis. PLoS Biol. **7**, e1000124.

Feng, S., Cokus, S.J., Zhang, X., Chen, P.Y., Bostick, M., Goll, M.G., Hetzel, J., Jain, J., Strauss, S.H., Halpern, M.E., et al. (2010). Conservation and divergence of methylation patterning in plants and animals. Proc. Natl. Acad. Sci. USA **107**:8689–8694.

Gilles, L.M., Khaled, A., Laffaire, J.B., Chaignon, S., Gendrot, G., Laplaige, J., Bergès, H., Beydon, G., Bayle, V., Barret, P., et al. (2017). Loss of pollen-specific phospholipase NOT LIKE DAD triggers gynogenesis in maize. EMBO J. **36**:707–717.

Hegarty, M.J., Barker, G.L., Wilson, I.D., Abbott, R.J., Edwards, K.J., and Hiscock, S.J. (2006). Transcriptome shock after interspecific hybridization in senecio is ameliorated by genome duplication. Curr. Biol. **16**:1652–1659.

Hochholdinger, F., and Baldauf, J.A. (2018). Heterosis in plants. Curr. Biol. **28**:R1089–R1092.

Jiang, C., Sun, J., Li, R., Yan, S., Chen, W., Guo, L., Qin, G., Wang, P., Luo, C., Huang, W., et al. (2022). A reactive oxygen species burst causes haploid induction in maize. Mol. Plant **15**:943–955.

Kaushal, P., Dwivedi, K.K., Radhakrishna, A., Srivastava, M.K., Kumar, V., Roy, A.K., and Malaviya, D.R. (2019). Partitioning apomixis components to understand and utilize gametophytic apomixis. Front. Plant Sci. **10**:256.

Kelliher, T., Starr, D., Richbourg, L., Chintamanani, S., Delzer, B., Nuccio, M.L., Green, J., Chen, Z., McCuiston, J., Wang, W., et al. (2017). MATRILINEAL, a sperm-specific phospholipase, triggers maize haploid induction. Nature **542**:105–109.

Khanday, I., Skinner, D., Yang, B., Mercier, R., and Sundaresan, V. (2019). A male-expressed rice embryogenic trigger redirected for asexual propagation through seeds. Nature **565**:91–95.

Kim, D., Langmead, B., and Salzberg, S.L. (2015). HISAT: a fast spliced aligner with low memory requirements. Nat. Methods **12**:357–360.

Li, X., Meng, D., Chen, S., Luo, H., Zhang, Q., Jin, W., and Yan, J. (2017). Single nucleus sequencing reveals spermatid chromosome fragmentation as a possible cause of maize haploid induction. Nat. Commun. **8**:991.

Liu, C., Li, X., Meng, D., Zhong, Y., Chen, C., Dong, X., Xu, X., Chen, B., Li, W., Li, L., et al. (2017). A 4-bp insertion at *ZmPLA1* encoding a putative phospholipase A generates haploid induction in maize. Mol. Plant **10**:520–522.

Liu, H., Wang, K., Jia, Z., Gong, Q., Lin, Z., Du, L., Pei, X., and Ye, X. (2020). Efficient induction of haploid plants in wheat by editing of *TaMTL* using an optimized *Agrobacterium*-mediated CRISPR system. J. Exp. Bot. **71**:1337–1349.

Marimuthu, M.P.A., Jolivet, S., Ravi, M., Pereira, L., Davda, J.N., Cromer, L., Wang, L., Nogué, F., Chan, S.W.L., Siddiqi, I., et al. (2011). Synthetic clonal reproduction through seeds. Science **331**:876.

Mieulet, D., Jolivet, S., Rivard, M., Cromer, L., Vernet, A., Mayonove, P., Pereira, L., Droc, G., Courtois, B., Guiderdoni, E., et al. (2016). Turning rice meiosis into mitosis. Cell Res. **26**:1242–1254.

Ozias-Akins, P., and Conner, J.A. (2020). Clonal reproduction through seeds in sight for crops. Trends Genet. **36**:215–226.

Ozias-Akins, P., and van Dijk, P.J. (2007). Mendelian genetics of apomixis in plants. Annu. Rev. Genet. **41**:509–537.

Pertea, M., Pertea, G.M., Antonescu, C.M., Chang, T.C., Mendell, J.T., and Salzberg, S.L. (2015). StringTie enables improved reconstruction of a transcriptome from RNA-seq reads. Nat. Biotechnol. **33**:290–295.

Sailer, C., Schmid, B., and Grossniklaus, U. (2016). Apomixis allows the transgenerational fixation of phenotypes in hybrid plants. Curr. Biol. **26**:331–337.

Tan, E.H., Henry, I.M., Ravi, M., Bradnam, K.R., Mandakova, T., Marimuthu, M.P., Korf, I., Lysak, M.A., Comai, L., and Chan, S.W. (2015). Catastrophic chromosomal restructuring during genome elimination in plants. Elife **4**, e06516.

Underwood, C.J., and Mercier, R. (2022). Engineering apomixis: clonal seeds approaching the fields. Annu. Rev. Plant Biol. **73**:201–225.

Underwood, C.J., Vijverberg, K., Rigola, D., Okamoto, S., Oplaat, C., Camp, R.H.M.O.d., Radoeva, T., Schauer, S.E., Fierens, J., Jansen, K., et al. (2022). A *PARTHENOGENESIS* allele from apomictic dandelion can induce egg cell division without fertilization in lettuce. Nat. Genet. **54**:84–93.

Wang, C., Liu, Q., Shen, Y., Hua, Y., Wang, J., Lin, J., Wu, M., Sun, T., Cheng, Z., Mercier, R., et al. (2019). Clonal seeds from hybrid rice by simultaneous genome engineering of meiosis and fertilization genes. Nat. Biotechnol. **37**:283–286.

Wang, K. (2020). Fixation of hybrid vigor in rice: synthetic apomixis generated by genome editing. aBIOTECH **1**:15–20.

Xie, E., Li, Y., Tang, D., Lv, Y., Shen, Y., and Cheng, Z. (2019). A strategy for generating rice apomixis by gene editing. J. Integr. Plant Biol. **61**:911–916.

Xu, C., Bai, Y., Lin, X., Zhao, N., Hu, L., Gong, Z., Wendel, J.F., and Liu, B. (2014). Genome-wide disruption of gene expression in allopolyploids but not hybrids of rice subspecies. Mol. Biol. Evol. **31**:1066–1076.

Yao, L., Zhang, Y., Liu, C., Liu, Y., Wang, Y., Liang, D., Liu, J., Sahoo, G., and Kelliher, T. (2018). *OsMATL* mutation induces haploid seed formation in *indica* rice. Nat. Plants **4**:530–533.